A $PtdInsP_3$- and Rho GTPase-mediated positive feedback loop regulates neutrophil polarity

Orion D. Weiner*†, Paul O. Neilsen‡, Glenn D. Prestwich§, Marc W. Kirschner*, Lewis C. Cantley†, and Henry R. Bourne¶#

*Department of Cell Biology, Harvard Medical School, 240 Longwood Ave/ C-1, Boston, MA 02115, USA
†Department of Cell Biology, Harvard Medical School, Division of Signal Transduction, Beth Israel Deaconess Medical Center, Boston, MA 02115, USA
‡Echelon Research Laboratories, 420 Chipeta Way, Suite 180, Salt Lake City, UT 84108
§Department of Medicinal Chemistry, University of Utah, 419 Wakara Way, Suite 205, Salt Lake City, UT 84108, USA
¶Department of Cellular and Molecular Pharmacology, University of California, San Francisco, CA 94143-0450, USA
#e-mail: bourne@cmp.ucsf.edu

Published online: 24 June 2002; DOI: 10.1038/ncb811

When presented with a gradient of chemoattractant, many eukaryotic cells respond with polarized accumulation of the phospholipid $PtdIns(3,4,5)P_3$. This lipid asymmetry is one of the earliest readouts of polarity in neutrophils, *Dictyostelium discoideum* and fibroblasts. However, the mechanisms that regulate $PtdInsP_3$ polarization are not well understood. Using a cationic lipid shuttling system, we have delivered exogenous $PtdInsP_3$ to neutrophils. Exogenous $PtdInsP_3$ elicits accumulation of endogenous $PtdInsP_3$ in a positive feedback loop that requires endogenous phosphatidylinositol-3-OH kinases (PI(3)Ks) and Rho family GTPases. This feedback loop is important for establishing $PtdInsP_3$ polarity in response to both chemoattractant and to exogenous $PtdInsP_3$; it may function through a self-organizing pattern formation system. Emergent properties of positive and negative regulatory links between $PtdInsP_3$ and Rho family GTPases may constitute a broadly conserved module for the establishment of cell polarity during eukaryotic chemotaxis.

By combining genetics and pharmacology to inhibit signalling cascades, we are beginning to understand the components that are necessary for directed cell polarity. However, the mechanisms through which these components interact to produce cell polarity are less well understood. Here, we focus on the role of the phospholipid $PtdInsP_3$ in the cell polarization process. This lipid has a strong polarity during chemotaxis of *Dictyostelium*[1,2], neutrophils[3] and fibroblasts[4]. The internal gradient of $PtdInsP_3$ exceeds that of the external chemoattractant gradient and is one of the most upstream signalling molecules known to do so during cell polarization[3]. Pharmacological, biochemical and genetic inhibition of $PtdInsP_3$ production interfere with cell polarity and chemotaxis in many systems[5–10]. Furthermore, $PtdInsP_3$ itself suffices to induce cell polarity and motility in neutrophils[11] and fibroblasts[12]. Thus, $PtdInsP_3$ occupies a privileged position as the most upstream molecule known to exhibit asymmetry during chemotaxis and one of the most downstream molecules that suffices to induce cell polarity and motility. To explore how this lipid regulates cell polarity, we have assessed the effects of delivering exogenous $PtdInsP_3$ to cells which contain an internal probe that allows the spatial distribution of PI(3)K lipid products to be determined.

$PtdInsP_3$ polarization during chemotaxis could result from the polarized activation of chemoattractant receptors or PI(3)Ks. Alternatively, it could reflect signals generated downstream of $PtdInsP_3$ production. To test the latter hypothesis, we sought to deliver exogenous $PtdInsP_3$ to neutrophils. $PtdInsP_3$ and other anionic phospholipids do not permeate the membranes of most cells. However, when complexed to cationic carriers, such as histone, phosphoinositides can be delivered to cells and exert physiological responses[13]. To assess the spatial distribution of PI(3)K lipid products, we used neutrophil-like differentiated HL-60 cells, which express PH-Akt–GFP (the pleckstrin homology domain of Akt tagged with green fluorescent protein), a fusion protein that specifically binds to $PtdInsP_3$ and $PtdIns(3,4)P_2$ (ref. 3). At early times (30–120 s) after incubation with C16-$PtdInsP_3$ (30 μM) complexed to histone (10 μM), cells exhibit ruffling and uniform translocation of PH-Akt–GFP to the plasma membrane (Figs 1a–d and 2b; 27 out of 59 cells translocated PH-Akt–GFP between 30 and 60 s). Lower

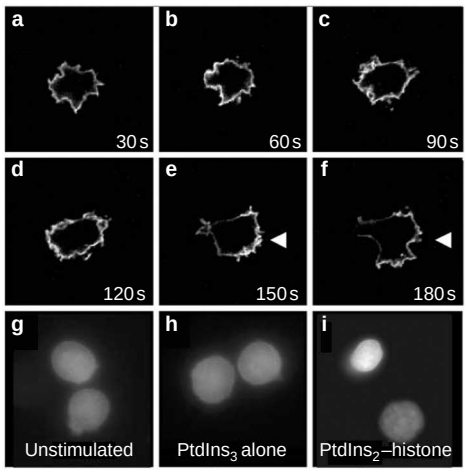

Figure 1 **$PtdInsP_3$–histone induces translocation of PH-Akt–GFP.** A spatial readout is shown for generation of $PtdInsP_3$ and $PtdIns(3,4)P_2$ at the plasma membrane in neutrophil-differentiated HL-60 cells. **a–f**, Time course of cells exposed to $PtdInsP_3$ (30 μM)–histone (10 μM). **g**, Unstimulated cells. **h**, Cells exposed to $PtdInsP_3$ (30 μM) without histone carrier. **i**, Cells exposed to $PtdIns(4,5)P_2$ (30 μM)–histone (10 μM).

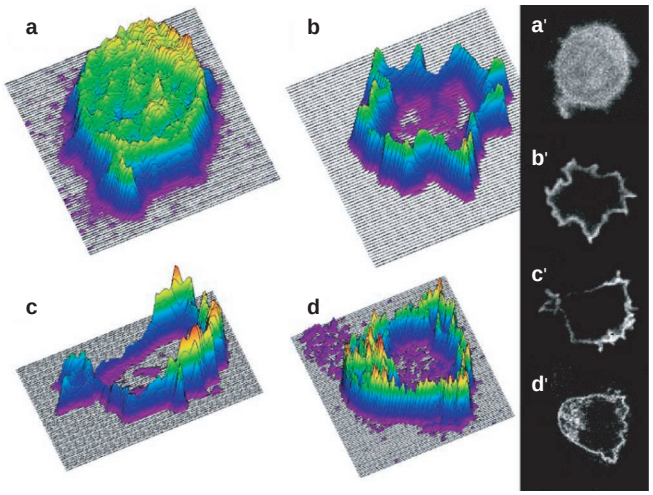

Figure 2 **Surface plots of PH-Akt–GFP distribution in neutrophil-differentiated HL-60 cells.** Height corresponds to fluorescence intensity of each pixel from confocal images of cells. **a**, An unstimulated cell. **b**, A cell stimulated with PtdInsP$_3$–histone for 30 s. **c**, A cell stimulated with PtdInsP$_3$–histone for 150 s. **d**, A cell expressing the chemokine receptor C5AR–GFP[14] stimulated with 100 nM FMLP for 150 s. **a′–d′**, Confocal images from which the surface plots in **a–d** were generated.

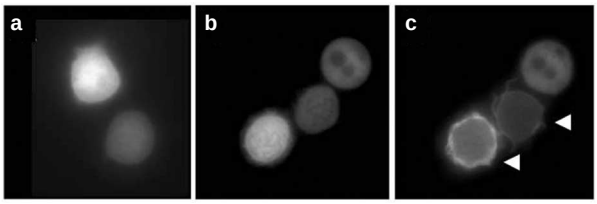

Figure 3 **PI(3)K and Rho GTPase inhibitors block PtdInsP$_3$–histone-induced PH-Akt–GFP translocation. a**, Cells treated with LY 294002 (200 μM) for 20 min and then stimulated with PtdInsP$_3$ (30 μM)–histone (10 μM). Similar doses of LY 294002 were needed to block phosphorylation of Akt in response to chemoattractant (see Supplementary Information, Fig. S2). **b**,**c**, Cells pretreated with *Clostridium difficile* toxin B (90 μg ml^{-1}) for 4–5 h and sequentially stimulated with PtdInsP$_3$–histone (**b**) and then insulin (**c**) to test for cell viability. In **c**, two of the three cells are viable, as judged by PH-Akt–GFP translocation in response to insulin (arrowheads).

concentrations of C16-PtdInsP$_3$ (10 μM) complexed to histone (3 μM) elicited approximately half this response (16 out of 74 cells translocated PH-Akt–GFP between 30 and 60 s).

Cells polarize after incubation with PtdInsP$_3$–histone for 2–3 min. Surprisingly, they also asymmetrically accumulate PH-Akt–GFP at the leading edge (Fig. 1e,f, arrowheads; also see Fig. 2c; 15 out of 55 cells showed polarized PH-Akt–GFP in this time frame) and migrate 1–2 cell diameters. These translocations can be observed most easily in the surface plots of Fig. 2. Polarity was usually maintained for 2–10 min. For almost all of the cells, the pattern of PH-Akt–GFP recruitment and polarization mirrored their actin rearrangements with the final polarized morphology, ranging from a more fibroblast-like crescent to the polarized cell pictured in Fig. 2e,f; the latter pattern is typical of the majority of polarized cells. The patterns of polarity closely resemble those seen with fMLP as the stimulus. Similar data was obtained using a PtdInsP$_3$ antibody (see Supplementary Information, Fig. S1). These data suggest that PtdInsP$_3$ can induce its own asymmetry. Unstimulated cells (Figs 1g and 2a) and cells incubated with PtdInsP$_3$ without a histone carrier (Fig. 1h) failed to induce translocation of PH-Akt–GFP. This suggests that the PtdInsP$_3$–histone effect is not mediated by an extracellular PtdInsP$_3$ receptor (2 out of 66 unstimulated cells and 2 out 58 cells stimulated with PtdInsP$_3$ alone translocated PH-Akt–GFP uniformly at 30–60 s; 0 out of 63 unstimulated cells and 0 out of 67 cells stimulated with PtdInsP$_3$ alone exhibited polarized PH-Akt–GFP recruitment at 2–3 min). This effect was not a general property of lipid–histone complexes, as PtdIns(4,5)P$_2$–histone failed to induce recruitment of PH-Akt–GFP (Fig. 1i; 5 out of 52 cells uniformly translocated PH-Akt–GFP in 30–60 sec, and 0 out of 56 cells exhibited polarized PH-Akt–GFP recruitment at 2–3 min. A GFP-tagged chemoattractant receptor[14] remained uniformly distributed throughout the plasma membrane in polarized cells, as previously described for neutrophils[14] and *Dictyostelium*[15]. This suggests that the PH-Akt–GFP asymmetry we observed after PtdInsP$_3$–histone stimulation is not a reflection of cell morphology (Fig. 2d). It is important to note that translocation of PH-Akt–GFP and polarization in response to PtdInsP$_3$–histone is less robust than that seen in response to an optimal dose of chemoattractant. This suggests that activated receptors stimulate production of more PtdInsP$_3$ than we are able to deliver to the cells exogenously, or that signalling from chemoattractant receptors provides signals to the cell polarization process in addition to PtdInsP$_3$.

To determine whether endogenous signalling cascades are necessary for the effects of PtdInsP$_3$–histone on cells, we analysed the consequences of inhibiting endogenous PI(3)Ks and Rho GTPases with a PI(3)K inhibitor (LY 294002) or *Clostridium difficile* toxin B (toxB), which inhibits the actions of Rac, Rho and Cdc42 GTPases. Pretreating cells with LY 294002 (200 μM for 20 min) completely prevented PtdInsP$_3$–histone from inducing PH-Akt–GFP translocation (Fig. 3a; 0 out of 89 cells responded by translocating PH-Akt–GFP). Wortmannin (200 nM) produces similar effects (data not shown). Approximately 70% inhibition was observed with 100 μM LY 294002 (10 out of 67 cells responded with PH-Akt–GFP translocation (data not shown)). Similar data was obtained using a PtdInsP$_3$ antibody instead of PH-Akt–GFP (see Supplementary Information, Fig. S1). These results suggest that the PH-Akt–GFP translocation observed after exposure of cells to PtdInsP$_3$–histone does not depend solely on exogenous PtdInsP$_3$, but rather that PtdInsP$_3$ cooperates with endogenous PI(3)Ks in a positive feedback loop that is necessary to generate enough PtdInsP$_3$ for a response. Although our data are most consistent with a positive feedback loop, we cannot rule out a purely permissive role for endogenous PI(3)K or basal PtdInsP$_3$ levels in the effects of exogenous PtdInsP$_3$–histone with these experiments. The concentrations of LY294002 and wortmannin needed to block PtdInsP$_3$-induced PH-Akt–GFP translocation are high when compared to doses of these inhibitors needed to block PI(3)K signalling in other cells, such as fibroblasts. However, these mirror the concentrations necessary to block Akt phosphorylation (see Note added in proof), PH-Akt–GFP translocation[3] and PtdInsP$_3$ antibody staining (F. Wang, personal communication) in HL-60 cells in response to chemoattractant stimulation. This suggests that these cells are relatively resistant to PI(3)K inhibitors. Intriguingly, at later times (greater than 5 min), some LY 294002-treated cells do show uniform translocation of PH-Akt–GFP to the plasma membrane (17 out of 122 cells exhibited this behaviour (data not shown)). This suggests that, given time, enough PtdInsP$_3$ can be delivered to the cells to generate PH-Akt–GFP translocation, even without a contribution from endogenous PI(3)Ks. However, these cells consistently failed to develop polarized PH-Akt–GFP distributions, (1 out of 17 cells showing translocation went on to polarize PH-Akt–GFP), suggesting that the PtdInsP$_3$ positive feedback loop is important for developing PtdInsP$_3$ polarity.

Similarly, pretreating cells with toxB prevented PtdInsP$_3$–histone from inducing PH-Akt–GFP translocation (Fig. 3b). Because

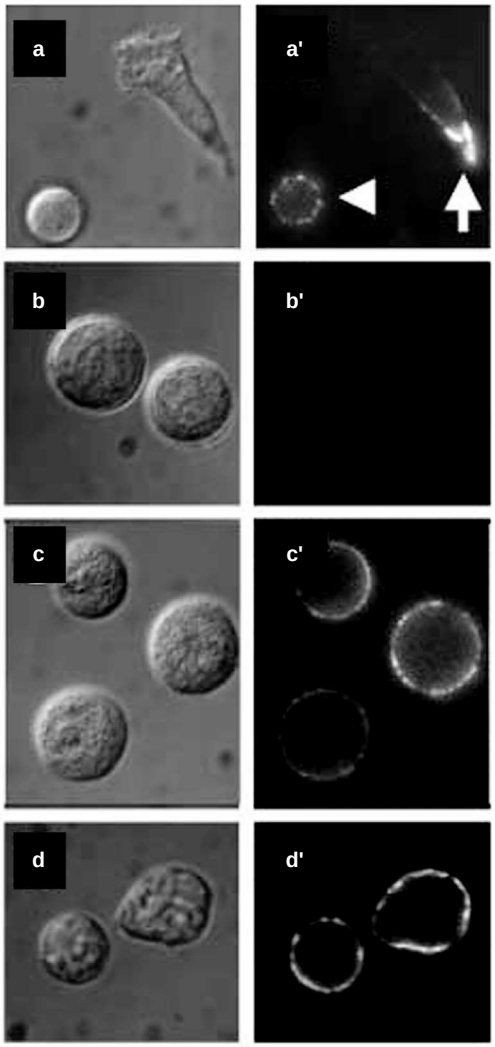

Figure 4 **Endogenous PI(3)K and Rho GTPases are not required for PtdInsP$_3$–histone uptake. a**, Control cells treated with fluorescent NBD–PtdInsP$_3$ (30 μM)–histone (10 μM) for 5 min. **b**, Cells treated with NBD–PtdInsP$_3$ (30 μM) without histone carrier. **c**, Cells pretreated with LY 294002 (200 μM) for 20 min and then exposed to NBD–PtdInsP$_3$ (30 μM)–histone (10 μM). **d**, Cells were pretreated with toxB and then exposed to NBD–PtdInsP$_3$ (30 μM)–histone (10 μM). **a**–**d**, Nomarski images. **a′**–**d′**, immunofluorescence images.

toxB also can induce cell lethality, we tested for cell viability by subsequently treating cells with insulin, which we previously demonstrated to induce Rho-GTPase-independent translocation of PH-Akt–GFP to the plasma membrane[3]. Only cells that translocated PH-Akt–GFP in response to insulin (Fig. 3c) were scored for their previous responsiveness to PtdInsP$_3$–histone; of 77 cells that exhibited PH-Akt–GFP translocation in response to insulin, none showed PH-Akt–GFP translocation in response to incubation with PtdInsP$_3$–histone. These data suggest that one or more Rho GTPases are necessary components of the PtdInsP$_3$–histone-induced PtdInsP$_3$ positive feedback loop. Rho GTPase inhibition also blocks PH-Akt–GFP translocation[3] and Akt activation (G. Servant and D. Stokoe, personal communication) in cells responding to chemoattractant, suggesting that a similar signalling cascade operates during chemotaxis.

The inhibitory effects of LY 294002 and toxB on responses to exogenous PtdInsP$_3$–histone treatment could result from inhibition of PtdInsP$_3$ delivery to the cells, rather than from inhibiting cooperation between exogenous PtdInsP$_3$ and endogenous signalling cascades. To discriminate between these possibilities, we analysed delivery of fluorescently derivatized NBD-PtdInsP$_3$–unlabelled histone to cells with and without inhibitors of PI(3)K and Rho GTPases. In control cells that failed to polarize, NBD–PtdInsP$_3$–histone was distributed uniformly at the cell periphery (Fig. 4a, arrowhead). By contrast, in cells that did polarize, NBD–PtdInsP$_3$ accumulated in the cell posterior (Fig. 4a, arrow). An important qualification of these results is that the fluorescent probe, located at the end of one of the phospholipid's fatty acid tails, is not destroyed by metabolism of the inositol headgroup. Consequently, the observed fluorescence reflects delivery of exogenous PtdInsP$_3$–histone to the cells, although it probably does not solely represent unmodified PtdInsP$_3$. Indeed, we never observe preferential accumulation of the PH-Akt–GFP at the trailing edge of polarized cells. Thus the NBD–PtdInsP$_3$ results suggest that accumulation of PH-Akt–GFP at the leading edge of polarized cells does not represent accumulation of exogenous PtdInsP$_3$–histone at this location. Delivery of NBD–PtdInsP$_3$ to the cell periphery depends on the presence of histones (Fig. 4b). Although treatment with LY 294002 (Fig. 4c) or toxB (Fig. 4d) prevents cell polarization, these agents do not inhibit delivery of exogenous NBD–PtdInsP$_3$ to the cell periphery. Taken together, the data suggest that these agents do not produce their effects by inhibiting the cellular uptake of PtdInsP$_3$–histone.

Discussion

These results, showing that translocation of PH-Akt–GFP to the plasma membrane in response to PtdInsP$_3$–histone requires endogenous PI(3)K activity and Rho GTPases, can be explained by postulating a positive feedback loop that involves PtdInsP$_3$ and the Rho GTPases. Such a feedback loop could explain paradoxical epistatic relations between Rho GTPases and PI(3)Ks identified in genetic, pharmacological and biochemical analyses: PI(3)K activity has been shown to function upstream of Rac and Cdc42 activation[16,17], but Rac and Cdc42 have been shown to function upstream of PtdInsP$_3$ generation[14,18–21]; this apparent paradox has sometimes been observed in the same cell, for example, in neutrophils[14,17] and T-cells[19]. Our findings suggest that these conflicting results may be explained by PtdInsP$_3$ and Rho GTPases functioning both upstream and downstream of one another in a positive feedback loop.

One question concerns how such a feedback loop contributes to cell polarity during chemotaxis. A possible clue comes from models of mechanisms by which developmental organizers form self-organizing patterns from small gradients or stochastic differences in signalling[22]. The first postulated ingredient of such pattern formation systems is a signal that amplifies itself in a short-range positive feedback fashion. We propose that the PtdInsP$_3$- and Rho GTPase-dependent positive feedback loop provides this function in eukaryotic chemotaxis. The second ingredient of this self-organizing pattern formation system[22] is that signals from the activator generate a more long-range inhibitor of signalling. Good candidates for this inhibitory function in eukaryotic chemotaxis include negative regulators of PtdInsP$_3$ accumulation, such as the lipid phosphatases PTEN (phosphatase and tensin homologue deleted on chromosome ten)[23,24] and SHIP (SH2-containing inositol phosphatase)[25], and negative regulators of Rho GTPase activation (for example, a recently identified negative feedback loop in *Saccharomyces cerevisiae*, in which Cdc42 induces phosphorylation and inactivation of its own guanine nucleotide exchange factor[26]). In addition to chemotaxis[22], pattern formation systems that are consistent with this general model (though not necessarily the same components) include hydra regeneration and retinotectal mapping. Good candidates for components in the positive feedback loop include: PtdInsP$_3$ activation of guanine nucleotide exchange factors for Rac, such as Prex[27], Cdc42/Rac-induced activation of PtdInsP$_3$

production through direct binding to the Rho GAP domain of the PI(3)K adapter p85 (refs 20,21,28) or induction of PI(4,5)P_2 generation through recruitment of PI(5)K[29], which could increase availability of substrate for PtdInsP_3 production by PI(3)Ks.

In summary, PtdInsP_3 asymmetries are observed during chemotaxis of many cells, from neutrophils[3] to *Dictyostelium*[1,2] to fibroblasts[4], and in response to very different stimuli, such as ligands for G-protein coupled receptors[1–3] and tyrosine kinase receptors[4], as well as direct delivery of PtdInsP_3, as we have shown. We propose that the emergent properties of positive and negative regulatory links between PtdInsP_3 and Rho GTPases constitute a broadly conserved module for establishing cell polarity during eukaryotic chemotaxis. Such a polarity module could account for the remarkable convergence of behaviour among these widely diverse cells and chemotactic stimuli. Important future directions include dissecting the wiring of the putative positive and negative feedback loops and developing better tools to spatially analyse and manipulate protein and lipid activities. This will allow us to gain a deeper understanding of how eukaryotic cells polarize and migrate in response to cues from the world around them.

Note added in proof: The data concerning the concentrations of PI(3)K inhibitors required to block Akt phosphorylation are included in the accompanying manuscript by Wang et al. Nature Cell Biol. *DOI:10.1038/ncb810.* □

Methods

Cell preparation

HL-60 cells expressing PH-Akt–GFP[3] were stimulated to differentiate, as described[3], except that endotoxin-free hybridoma-tested dimethyl sulphoxide (D2650; Sigma, St Louis, MO) was used. Treatment with LY 294002 and toxB were performed as described[3], except that LY 294002 was continuously incubated with the cells for LY 294002 treatment.

Lipid delivery

Long chain (Di-C_{16}) synthetic phospholipids (Echelon, Salt Lake City, UT) were freshly prepared at 300 μM in 150 mM sodium chloride, 4 mM potassium chloride and 20 mM Hepes at pH 7.2, and resuspended by bath sonication or vigorous vortexing. Histone–phospholipid complexes were prepared by incubating 300 μM phospholipids with 100 μM freshly prepared histone (Echelon), vortexed vigorously, incubated for 5 min at room temperature and diluted 1:10 with modified Hanks buffered saline solution[30] immediately before addition to HL-60 cells in suspension. Cells were immediately added to an agarose-lined coverslip using wide-bore pipette tips[30].

Microscopy

Images were acquired with an epifluorescence microscope (Nikon, Melville, NY)and an axiovert confocal microscope (Zeiss, Woburn, MA). Quantitation of PH-Akt–GFP translocation and cell polarization were performed on random fields of living cells for a minimum of 3 independent experiments. We defined polarization as Akt recruitment continuously covering 25–75% of the cell surface. Cells with two independent fronts were not counted as polarized. Surface plots for Fig. 2 were generated from confocal images using NIH Image1.62.

RECEIVED 23 JANUARY 2002; REVISED 5 APRIL 2002; ACCEPTED 30 APRIL 2002; PUBLISHED 24 JUNE 2002.

1. Meili, R. *et al. EMBO J.* **18,** 2092–2105 (1999).
2. Jin, T., Zhang, N., Long, Y., Parent, C. A. & Devreotes, P. N. *Science* **287,** 1034–1036 (2000).
3. Servant, G. *et al. Science* **287,** 1037–1040 (2000).
4. Haugh, J. M., Codazzi, F., Teruel, M. & Meyer, T. *J. Cell Biol.* **151,** 1269–1280 (2000).
5. Niggli, V. & Keller, H. *Eur. J. Pharmacol.* **335,** 43–52 (1997).
6. Vanhaesebroeck, B. *et al. Nature Cell Biol.* **1,** 69–71 (1999).
7. Funamoto, S., Milan, K., Meili, R. & Firtel, R. A. *J. Cell Biol.* **153,** 795–810 (2001).
8. Hirsch, E. *et al. Science* **287,** 1049–1053 (2000).
9. Li, Z. *et al. Science* **287,** 1046–1049 (2000).
10. Sasaki, T. *et al. Science* **287,** 1040–1046 (2000).
11. Niggli, V. *FEBS Lett.* **473,** 217–221 (2000).
12. Derman, M. P. *et al. J. Biol. Chem.* **272,** 6465–6470 (1997).
13. Ozaki, S., DeWald, D. B., Shope, J. C., Chen, J. & Prestwich, G. D. *Proc. Natl Acad. Sci. USA* **97,** 11286–11291 (2000).
14. Servant, G., Weiner, O. D., Neptune, E. R., Sedat, J. W. & Bourne, H. R. *Mol. Biol. Cell* **10,** 1163–1178 (1999).
15. Xiao, Z., Zhang, N., Murphy, D. B. & Devreotes, P. N. *J. Cell Biol.* **139,** 365–374 (1997).
16. Hawkins, P. T. *et al. Curr. Biol.* **5,** 393–403 (1995).
17. Benard, V., Bohl, B. P. & Bokoch, G. M. *J. Biol. Chem.* **274,** 13198–13204 (1999).
18. Yang, F. C. *et al. Immunity* **12,** 557–568 (2000).
19. Genot, E. M. *et al. Mol. Cell Biol.* **20,** 5469–5478 (2000).
20. Zheng, Y., Bagrodia, S. & Cerione, R. A. *J. Biol. Chem.* **269,** 18727–18730 (1994).
21. Bokoch, G. M., Vlahos, C. J., Wang, Y., Knaus, U. G. & Traynor-Kaplan, A. E. *Biochem. J.* **315,** 775–779 (1996).
22. Meinhardt, H. & Gierer, A. *Bioessays* **22,** 753–760 (2000).
23. Lilienthal, J. *et al. Curr. Biol.* **10,** 401–404 (2000).
24. Stambolic, V. *et al. Cell* **95,** 29–39 (1998).
25. Liu, Q. *et al. Genes Dev.* **13,** 786–791 (1999).
26. Gulli, M. *et al. Mol. Cell* **6,** 1155–1167 (2000).
27. Welch, H. C. E. *et al. Cell* **108,** 809–821 (2002).
28. Tolias, K. F., Cantley, L. C. & Carpenter, C. L. *J. Biol. Chem.* **270,** 17656–17659 (1995).
29. Carpenter, C. L., Tolias, K. F., Couvillon, A. C. & Hartwig, J. H. *Adv. Enzyme Regul.* **37,** 377–390 (1997).
30. Weiner, O. D. *et al. Nature Cell Biol.* **1,** 75–81 (1999).

ACKNOWLEDGEMENTS

We thank S. Ozaki and J. Chen for NBD–PtdInsP_3 synthesis, C. Kelley and M. Warny for the kind gift of *Clostridium difficile* toxin B, R. Tsien's lab for the PtdInsP_3-AM used in early experiments, V. Niggli for advice on using this compound with neutrophils, F. Wang for protocols for the PtdInsP_3 antibody, Echelon for the gift of phospholipids and histones, and C. Bargmann, C. Carpenter and C. Kenyon for helpful discussions. This work was in part supported by grants from the National Institutes of Health to H.R.B., L.C.C. (GM41890), M.W.K. (GM26825), P.O.N. (GM62734-03), and G.D.P. (NS29632). O.D.W. was supported by a Howard Hughes Medical Institute predoctoral fellowship and the Damon Runyon Cancer Research Fund.

Correspondence and requests for material should be addressed to H.R.B.

Supplementary Information is available on *Nature Cell Biology*'s website (http://cellbio.nature.com).

COMPETING FINANCIAL INTERESTS

The authors declare that they have no competing financial interests.

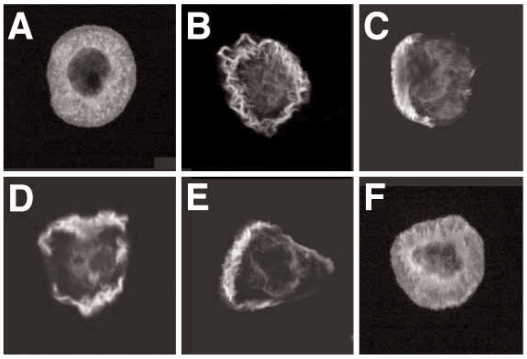

Figure S1 PIP_3 antibody staining of fMLP and PIP_3/histone stimulated neutrophil-like differentiated HL-60 cells. (A) Unstimulated cell. (B) Cell stimulated with 100 nM FMLP for 30 seconds. (C) Cell stimulated with 100 nM FMLP for 2 min. (D) Cell stimulated with PIP_3 (30 μM)/histone (10 μM) for 1 min. (E) Cell stimulated with PIP_3 (30 μM) / histone (10 μM) for 3 min. (F) Cell pretreated with 200 μM LY 294002 for 20 min and then stimulated with PIP_3 (30 μM) / histone (10 μM) for 1 min

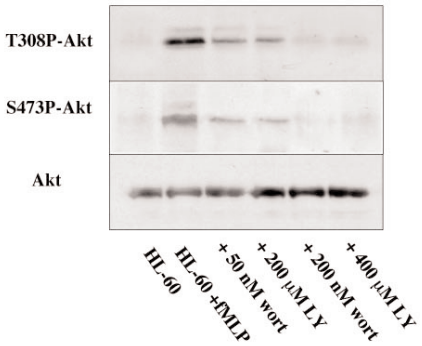

Figure S2 Inhibition of AKT phosphorylation in differentiated HL-60 cells by wortmannin and LY 294002. (B) Immunoblotting analysis of S473- and T308-phosphorylated Akt/PKB (S473P-AKT and T308P-AKT) in differentiated HL-60 with (HL-60 + fMLP, 1 min post-stimulation) or without stimulation by 100 nM fMLP (HL-60), and cells pretreated with various concentrations of wortmannin and LY 294002 and thereafter stimulated with fMLP. The level of total Akt/PKB was used as a measure of loading. These data are from a representative experiment of at least three performed with similar results. The data for Supplementary Figure 2 are controls from a separate paper (Fei Wang et al., submitted).

Supplementary methods

Immunoblots

Differentiated HL-60 cells were washed once with RPMI 1640/25 mM HEPES, resuspended in mHBSS, and thereafter stimulated with 100 nM fMLP. After stimulations, cells were lysed in RIPA buffer [1% Nonidet P-40, 0.5% deoxycholate, 0.2% SDS, 150 mM sodium chloride, 50 mM Tris-HCl (pH 7.4) containing 1 mM diisopropyl fluorophosphate and a cocktail of protease and phosphatase inhibitors. Equal amounts of protein lysates were loaded on reducing Laemmli gels, immunoblotted with antibodies against total AKT and phosphorylated AKT, detected with an ECL system (Pierce).

PI(3,4,5)P3 immunostaining

Differentiated HL-60 cells were stimulated with a uniform concentration of chemoattractant or PIP_3/histone and fixed for 20 min with 3.7% formaldehyde in cytoskeleton (CSK) buffer containing 10 mM HEPES, pH 7.2, 138 mM KCl, 3 mM $MgCl_2$, 2 mM EGTA, and 0.32 M sucrose. Cells were then washed twice in CSK, permeabilized with CSK buffer lacking sucrose and containing 0.2% triton X-100, and incubated for 30 min in a blocking solution (blotto) containing 50 mM Tris-HCl, pH 7.5, 1 mM $CaCl_2$, and 3% dry milk, followed by 1 hr incubation with an Echelon monoclonal anti-$PI(3,4,5)P_3$ antibody (in blotto). After three successive washes in a solution containing 25 mM Tris-HCl, pH 7.4, 140 mM NaCl, 2.5 mM KCl, and 1 mM $CaCl_2$, the cells were incubated with TxRed-conjugated goat anti-mouse IgM (1:400 dilution in blotto) for 45 min. They were then washed three times and mounted in Vectashield. Images were acquired on a Nikon TE300 microscope with a PerkinElmer Spinning Disk Confocal using a 63x1.4NA lens.